Confinement of 'Improved H-Modes' in the All-Tungsten ASDEX Upgrade

J. Schweinzer 1), A.C.C. Sips 2), G. Tardini 1), D. Told 1), R. Fischer 1), J.C. Fuchs 1), O. Gruber 1), J. Hobirk 1), F. Jenko 1), A. Kallenbach 1), R. M. McDermott 1), R. Neu 1), T. Pütterich 1), S. K. Rathgeber 1), M. Schneller 1), J. Stober 1) and the ASDEX Upgrade Team

1) Max-Planck-Institut für Plasmaphysik, D-85748 Garching, Germany, Euratom Association
2) EFDA-JET, Culham Science Centre, OX14 3DB, Abingdon, UK

E-mail contact of main author: josef.schweinzer@ipp.mpg.de

Abstract. The compatibility of improved H-modes in the all-W AUG with an unboronized wall was demonstrated, achieving H_{98}=1.18 and β_N =2.5 at triangularities $\delta < 0.35$. With boronization the light impurities and the radiated power fraction in the divertor were reduced, requiring N_2 seeding. The impurity seeding does not only protect the divertor tiles but also considerably improves the performance of improved H-mode discharges by up to 25%. The energy confinement increases to H_{98}-factors > 1.3 and thereby exceeds the best values in the carbon-dominated AUG at the same density and collisionality. This improvement is due to higher temperatures rather than to peaking of the electron density profile. Higher temperatures are reached at the pedestal top leading via profile stiffness without visible enhancement of R/L_{Ti} in the plasma core to an increase of the total plasma pressure. This picture is supported by non-linear gyro-kinetic GENE simulations.

1. Introduction

'Improved H-mode' discharges (IPHM) in ASDEX Upgrade (AUG) are characterized by enhanced confinement factors H_{98}>1, improved MHD-stability, a total beta β_N = 2 - 3.5 and a q-profile with a broad region in the plasma core of ~ zero shear and a q(0)≈1 [1]. This scenario, which is also often called Hybrid scenario, opens the way in ITER to either longer plasma pulse duration at reduced plasma current and Q=10 or to improved performance with Q>10 at full plasma current. Hybrid scenarios typically require moderate additional heating during the plasma current ramp-up to allow the formation of an adequate current profile (low central shear) in preparation for strong heating during the flat-top phase. This current ramp-up phase is thought to be crucial for improved H-mode operation. However, alternative current ramp-up scenarios were discovered such as an explicit 'late heating' scheme with a long ohmic phase at low plasma density before adding auxiliary heating. Surprisingly this resulted in better energy confinement compared with the 'early heating' scheme, with the discharge evolving to have low magnetic shear in the core during the high beta phase by means of the edge bootstrap current [1].

One of the major goals of the AUG tungsten programme has been to demonstrate the compatibility of such high performance scenarios with an all-W inner wall. Beginning in 1999, the plasma facing components (PFCs) in AUG have been changed in a stepwise manner from carbon to tungsten coated tiles [2]. In the reporting period of 2008-9[1)] all PFCs were coated with tungsten.

2. Comparison of IPHM in the all-W AUG with results from previous campaigns

During the last decade improved H-mode operation at AUG has been achieved for a wide range of deuterium plasmas using predominantly neutral beam injection (NBI) with heating powers up to 15MW. However, in order to obtain stationary conditions in AUG with its W-coated tiles, the W concentration in the plasma needs to be controlled. In an H-mode, the edge transport barrier provides a zone of good confinement, and the inward transport of tungsten is regulated by the ELMs. Thus, a higher ELM frequency is beneficial for reducing the tungsten

[1] In 2010 AUG is in a shutdown phase for the installation of internal coils. Operation will resume in Oct. 2010.

concentration [3]. The ELM frequency increases with the amount of additional heating, the edge q_{95} and the applied gas puff level. However, too high levels of fuelling deteriorate the global energy confinement. Thus, optimization of the plasma performance implies a control of the W concentration, while maintaining good confinement. In the core of the plasma, the neo-classical inward flow of W can lead to accumulation of tungsten which is caused by density peaking at high confinement conditions. Therefore, central heating needs to be provided by NBI and RF heating to produce sufficient central heat flux to enhance the turbulent transport in the plasma centre [4]. In particular in the all-W AUG a careful combination of these tools (gas puff and localized central heating) is a prerequisite to achieve stable operation with tolerable core W concentration below 5×10^{-5}. The mandatory gas puffing in the all-W AUG results in an operation at higher densities / collisonalities compared to earlier campaigns with a carbon dominated wall or during the transition phase (2001- 2006) with an incomplete W coverage (see fig. 1 - 3).

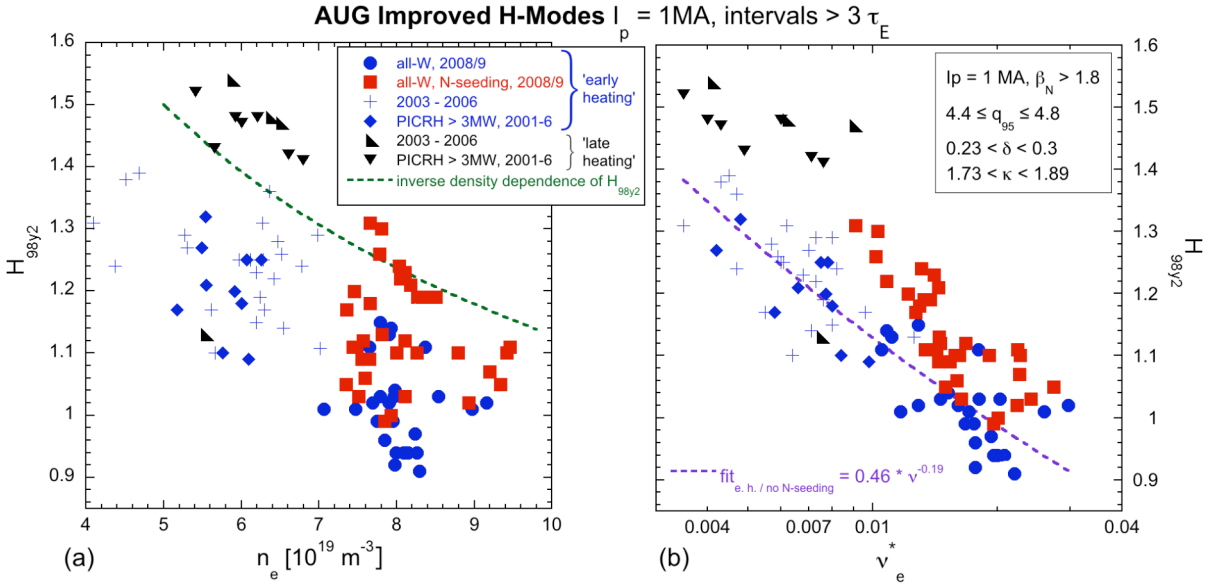

FIG. 1. H-mode confinement enhancement factor $H_{98(y,2)}$ dependence on (a) line-averaged density and (b) collisionality for 'early' (blue and red symbols) and 'late' heated (black symbols) improved H-mode discharges with plasma currents of 1MA at small/medium triangularity with a q_{95}~ 4.6.
The data have a total additional heating power between 5–15MW. Discharges from the 2008/9 campaigns are with D_2 fuelling ($1.0 \cdot 10^{21}$ – $1.2 \cdot 10^{22}$ s^{-1}) while discharges from 2003 to 2006 have no gas fuelling except a single one ($7 \cdot 10^{21}$ s^{-1}, H_{98y2}=1.1, $n_e = 7 \cdot 10^{19}$ m^{-3}). In 2008/9 all discharges use the early heating approach and have at least 0.8MW of ECRH power. The blue full circles refer to operation without N_2 seeding, while the red points are with N_2 seeding. IPHMs with high level of ICRH power (>3MW) are indicated as well. The results of the 2008/9 all-W campaigns are at higher plasmas density compared to previous campaigns. The envelope of H-factors for early heated IPHMs follows approximately a curve representing the inverse density behaviour of the H-mode scaling. Late heated IPHMs show better confinement than the early heated ones. In the right plot a fit to all early heated IPHMs without N_2 seeding is shown. Almost all N_2 seeded data points are above this curve demonstrating the improved confinement found by N_2 puffing, introduced for divertor protection. Low collisionality values of previous campaigns are so far not accessible in the all-W AUG.

In all of the campaigns between 2001 and 2006 ion cyclotron resonance heating (ICRH) was applied at 30 or 36 MHz using a hydrogen minority heating scheme with a maximum coupled power of 6MW. During AUG's transition phase from a carbon to a W machine ICRH was a very effective central heating method. The use of ICRF heating in the all-W AUG is now hampered by ICRF-related impurity sources from W-coated plasma facing components close

to the antennas [5]. Since the installation of W-coated antenna limiters, ICRF heating is accompanied by a strong W release, which obliterates the beneficial effect of central heating. Therefore, ICRH was not applied to IPHMs in 2008/9 and ECRH remains the only RF heating method available to supply the required central heating for the suppression of central W accumulation. The ECRH system on AUG is currently being upgraded to include four new 1MW/10s gyrotrons with frequencies at 105 and 140 GHz. One such new, long pulse (10s) gyrotron was available during 2008/9. The four older units which provide 500kW / 2s each have been available as well. Central deposition with the 140 GHz gyrotrons restricted the operation to magnetic fields B_t between 2.45T and 2.55T and to central densities n_e below $1.2 \cdot 10^{20}$ m^{-3}. The application of ECRH at 105GHz and B_t=2T was not an attractive option due to the even lower cut-off density ($7 \cdot 10^{19}$ m^{-3}) for 2nd harmonic X-mode (X2) heating. In order to allow AUG operation at lower q_{95} values (B_t values of 1.7T to 1.8T) 140 GHz ECRH using the 3rd harmonic X-mode (X3) was successfully developed [6] (see fig. 3).

At the end of April 2008, after a two year period without using boronization as a conditioning technique, AUG was boronized again. This led, as expected, to a clear reduction of the concentration of light impurities such as carbon and oxygen (C: 0.1-1%, O < 0,1%). The radiated power decreased, especially in the divertor, and the thermal load on the W-coated divertor tiles reached values of over 10 MW/m^2 [7], which is beyond the power handling capabilities of W coatings. As a consequence discharges in the boronized AUG with heating power above 10MW could be conducted in a safe manner only with active cooling of the divertor plasma by enhancing the radiation with N_2 seeding. The amount of puffed N_2 is feedback controlled by requesting a low divertor temperature, which is estimated by measuring the thermo-electric currents in the divertor [8]. As a positive surprise it turned out that puffing nitrogen does not only protect the divertor tiles, but also enhances significantly the confinement of the discharge [4]. The performance improvement with nitrogen seeding is very reproducible, holds for all D_2 fuelling rates under both freshly boronized and unboronized conditions, and enhances the energy confinement by up to 25%.

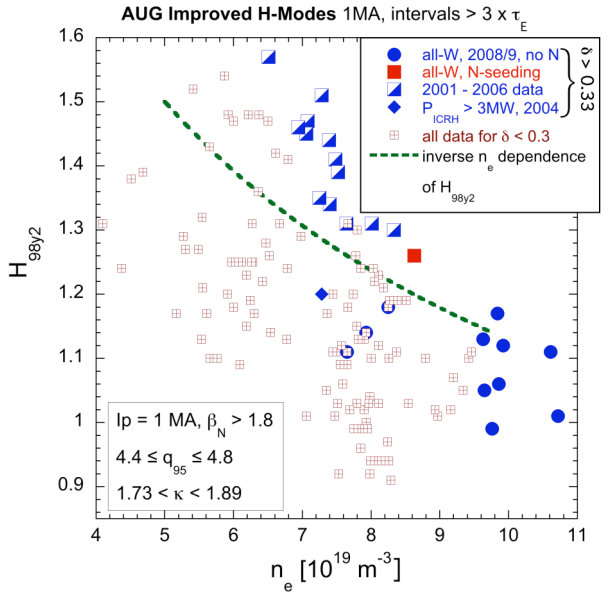

FIG. 2. Extension of FIG. 1a toward higher triangularity δ > 0.3. While the 2001-2006 high δ results show even better performance than the late-heated low δ IPHMs, results from the all-W AUG (no N_2, blue, full symbols) extend the density range to Greenwald fractions > 0.8. The single high δ data point with N_2 seeding (red symbol, D_2 puff $7 \cdot 10^{21}$ s^{-1}, after boronisation) fits well to the best results achieved in previous campaigns. Non-seeded discharges from the 2008/9 campaigns are with D_2 fuelling ($2.0 \cdot 10^{21} - 1.7 \cdot 10^{22}$ s^{-1}) while discharges from earlier campaigns have only small gas fuelling rates $0 - 1.6 \cdot 10^{21}$ s^{-1}. All high δ discharges are 'early heated'.

After damaging one of three flywheel generators in April 2006, operation in 2008 and most of 2009 was restricted to plasma currents $I_P \leq 1.2$ MA, low triangularity < 0.29, and input power less than 13 MW. Under these conditions only IPHMs utilizing the early heating scheme could be conducted in 2008/9. Only during the last three months of the 2009 campaign all three flywheel generators were available, which allowed the plasma shape to be increased up to ITER relevant values of δ~ 0.4 just for a few discharges (see fig. 2). Operation in this phase was hampered by insufficient levels of ECRH power.

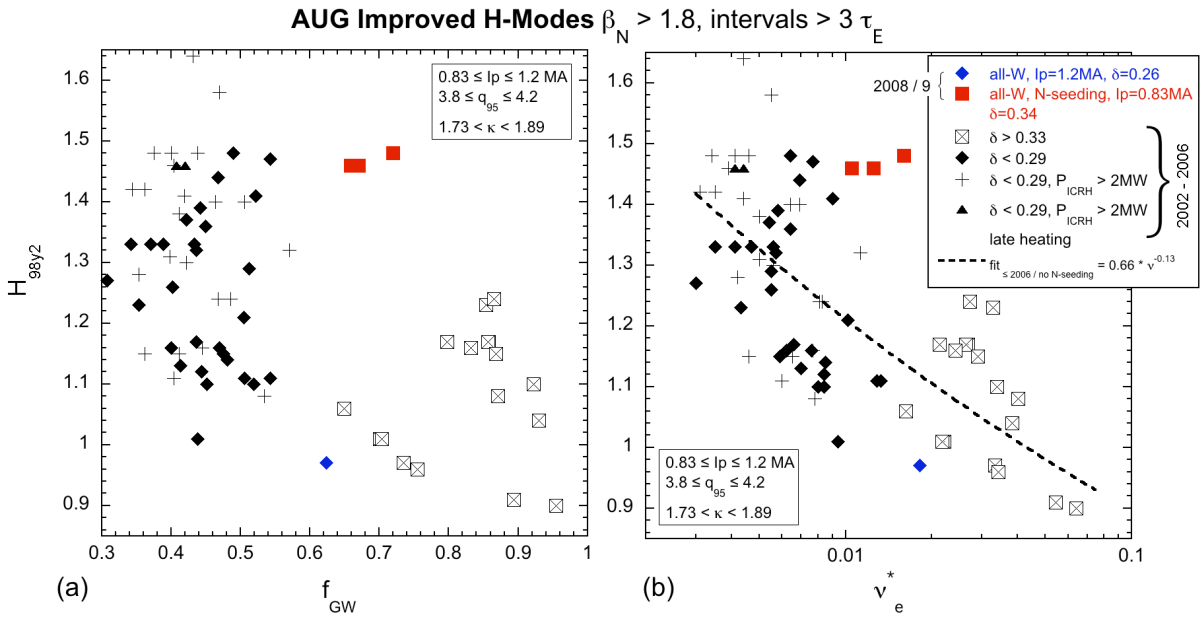

FIG. 3. H-mode confinement enhancement factor $H_{98(y,2)}$ dependence on (a) Greenwald fraction f_{GW} and (b) collisionality for 'early' and 'late' heated (black triangles) improved H-mode discharges with plasma currents 0.8 – 1.2MA at various triangularities with a safety factor around 4.0. The total additional heating power varies between 5–15MW.
While discharges from 2002 to 2006 at low δ have low D_2 gas fuelling rates ($0 – 5.0 \cdot 10^{21}$), the high δ discharges were puffed with rates $\geq 10^{22}$ s^{-1}. Late heated IPHMs show similar confinement than the early heated ones. IPHMs with high level of ICRH power (>2MW) are indicated as well.
Four discharges (blue and red symbols) from the 2008/9 all-W campaigns are shown in comparison with results form previous campaigns (black symbols). 2008/9 IPHMs use the early heating approach and have at least 0.7MW of ECRH power. The blue symbol (I_p=1.2MA, low δ, $D_2 = 9.4 \cdot 10^{21}$ s^{-1}) refers to operation without N_2 seeding, while the red points are with N_2 seeding (I_p = 0.83MA, B_T = 1.8T, high δ, $D_2 = 3.8 \cdot 10^{21}$ s^{-1}, with 140 GHz ECRH in X3 mode). The red data points seem to break the typical degradation of confinement with increasing f_{GW} or ν^*. In the right overview plot a fit to all IPHMs without N_2 seeding is shown. The confinement improvement caused by N_2 seeding seems to be even more pronounced than in the case of q_{95} = 4.6 (see fig. 1).

Fig. 1 - 3 show IPHM data from 2008/9 all-W campaigns for $q_{95} \sim 4.6$ (fig. 1: $\delta < 0.3$, fig. 2: $\delta > 0.3$) and $q_{95} \sim 4.0$ (fig. 3) operation, respectively, in comparison with similar discharges of previous campaigns. Each data point represents an average over a phase around the highest W_{MHD_max} ($W_{MHD} > 0.85 \cdot W_{MHD\_max}$) of a single discharge. Such high performance phases have to last at least for three energy confinement times, τ_E. A volume averaged definition of ν_e^* has been used in fig. 1 & 3 involving the thermal stored energy W_{th} rather than explicit temperature values. Most discharges in 2008/9 were conducted in one operational domain (fig. 1: $q_{95} \sim 4.6$ / $\delta < 0.3$, I_p= 1MA). Operation at higher δ and lower q_{95} was hampered by the aforementioned technical limitations (missing generator power, insufficient ECRH power and ICRF impurity generation). In the figures 1 - 3 no distinction has been made between boronized and unboronized wall. Keeping in mind the high values of n_e, f_{GW}, ν_e^* necessary to achieve stable operation with the all-W AUG, the performance of the 2008/9 N_2 seeded IPHMs is at least as good as in the carbon dominated era, for this parameter range.

3. Nitrogen seeded Improved H-Modes

In order to study the effect of N_2 seeding on energy confinement, discharges with zero N_2 puffing were followed by N_2 seeded ones without changing any other parameter. Time traces

and radial profiles for such a pair of comparable discharges are given in fig. 4 and fig. 5, respectively. The chosen pair of discharges were performed during a period in which no boronization for wall conditioning had been applied, but the behaviour presented in fig. 4 and fig. 5 is also typical for the boronized AUG. The major difference between boronized and non-boronized conditions is the resulting N_2 puff rate used under feedback in real-time to maintain a preset value of the divertor temperature. The N_2 puff rate controlled by this feedback system is lower in the non-boronized case, where edge and divertor radiation by intrinsic impurities is higher, as compared to conditions with freshly boronized walls.
With the introduction of N_2 a clear increase in stored energy W and in H_{98} is observed which is strongest in the phase with the highest applied heating power. This is typical for IPHM discharges where the H_{98} factor increases with β_N [9]. Similar neutron rates (not shown) are found in comparable discharges with and without N_2 puff. The higher plasma temperature (for the same input power) in the N_2 case compensates the loss in neutron yield due to increased D_2 dilution in the case with N_2 seeding, leading to a similar neutron rate [10]. Within the resolution of the MSE diagnostic q-profiles for comparable discharges with and without N_2 are identical.
Very similar line-averaged densities (see fig. 4) in both discharges suggest that the rise in stored energy in the presence of N_2 is mainly due to higher temperatures. Radial profiles of the latter are plotted in fig. 5.

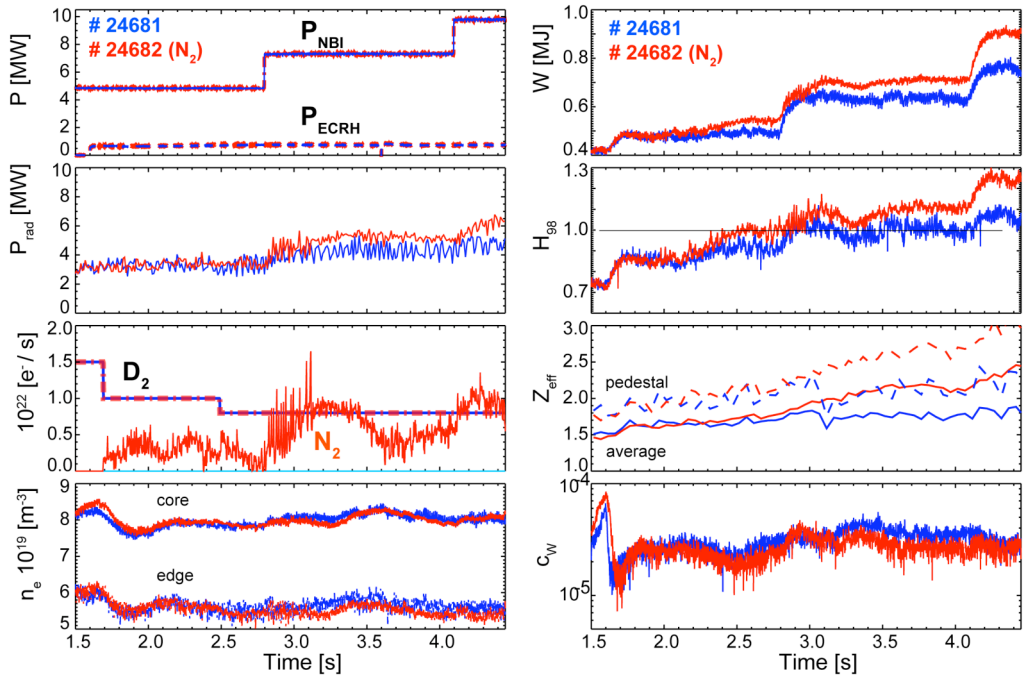

FIG. 4. Time traces of various parameters for two consecutive discharges (non-boronized AUG, I_p=1MA, B_t=2.5T, q_{95}=4.6, δ=0.29) with (#24682, red) and without (#24681, blue) N_2 seeding. The N_2 puff rate is feedback controlled to keep a preset divertor temperature (not shown). All discharge parameters are kept the same for both discharges, except to the introduction of N_2 in the case of #24682. Stored energy W, H factor H_{98}, total radiation P_{rad} and Z_{eff} (line averaged and pedestal value) increase with the applied N_2 puff, while other parameters like neutron yield (not shown), line-averaged density n_e and tungsten concentration c_W remain the same.

Gyrokinetic calculations (c.f. section 4) identify the Ion Temperature Gradient (ITG) driven mode as the dominant instability in the plasma core. Under these circumstances, profile stiffness has to be expected, so that the inverse gradient length $R/L_T = R \cdot |\nabla T|/T$ (of electrons and ions) is constrained near its critical value [11]. Moving from the pedestal top inwards, R/L_{T_j} is, within experimental uncertainties, the same in both discharges, as can be

seen in fig. 5 with its logarithmic scale. Therefore, the overall confinement improvement is mainly due to the higher pedestal temperatures, extending to the core via profile stiffness. The pedestal kinetic profiles for the presented pair of discharges can be found in [11].
In fig. 6 electron temperature and density values close to the pedestal top (ρ_{pol} = 0.9) are plotted for a set of discharges similar to the presented pair #24681/#24682. While the range of pedestal densities is not affected at all by the introduction of N_2, the pedestal electron temperature T_e of N_2 seeded discharges is considerably higher than in the unseeded case. A similar effect has been found for T_i.
The density profile is slightly more peaked in the presence of N_2, but not enough to contribute significantly to the observed improved energy confinement. This is a major difference to other regimes with improved confinement following impurity seeding (TEXTOR: RI-Mode [12] and AUG: CDH-Mode [13]) where n_e peaking was a dominant contributor to the confinement improvement.

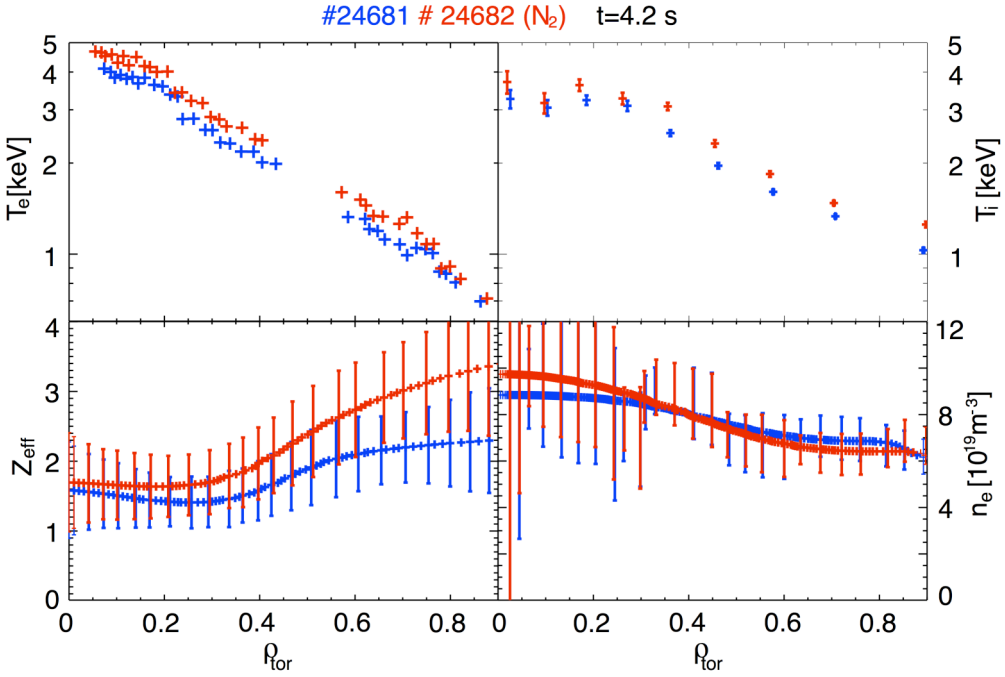

FIG. 5. Radial profiles during the high power phase (t=4.2s) of two comparable IPHM discharges (non-boronized AUG, I_p=1MA, B_t=2.5T, q_{95}=4.6, δ=0.29) with (#24682, red) and without (#24681, blue) N_2 seeding.

In fig. 5 the Z_{eff} profiles are also plotted. The concept of Integrated Data Analysis (IDA) within the framework of Bayesian probability theory was applied to determine the Z_{eff} profiles by combined analysis of background emission measured by the CXRS diagnostic and bremsstrahlung data [14]. The observed changes of the radial Z_{eff} profile by the introduction of N_2 suggest a hollow nitrogen density, which still needs to be confirmed by CXRS nitrogen density profile measurements. Such hollow N_2 profiles mean pronounced D_2 dilution at the edge transport barrier and almost no D_2 dilution in the plasma core. For the D ion channel the high dilution at the plasma edge caused by nitrogen ions opens the way for higher ion temperatures at the same pedestal top pressure as in the unseeded case. In combination with less dilution in the core and the well-established stiffness of T_i profiles a higher total ion pressure of N_2 seeded IPHMs (i.e. improved confinement) can be understood. However, the electron channel is also affected by the introduction of N_2 and higher electron pressure at the pedestal top (see fig. 6) was observed in the seeded case. Why the introduction of nitrogen leads to a higher pedestal pressure in the electron channel is not clear at the moment and will be the target of future investigations.

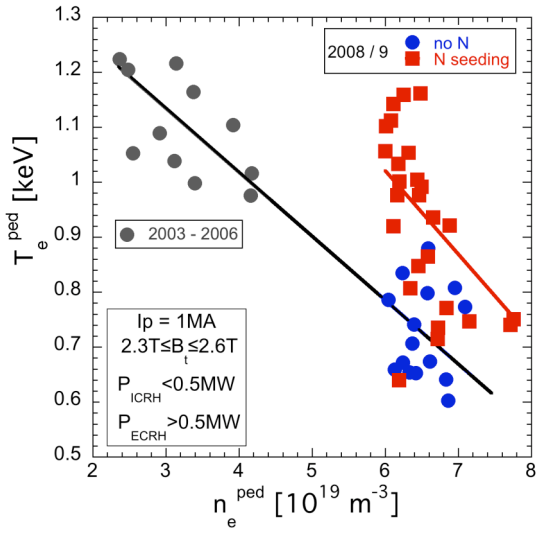

FIG. 6. Electron temperature and density values close to the pedestal top (ρ_{pol} = 0.9). All results of the 2008/9 all-W campaigns are at densities above 5.5 · 10^{19} m^{-3} and well separated from the lower ones of previous campaigns (grey symbols). Puffing of N_2 (red symbols) does not change the typical pedestal density of IPHMs, but increases the temperature. This indicates an increase of the electron pressure at the pedestal top.

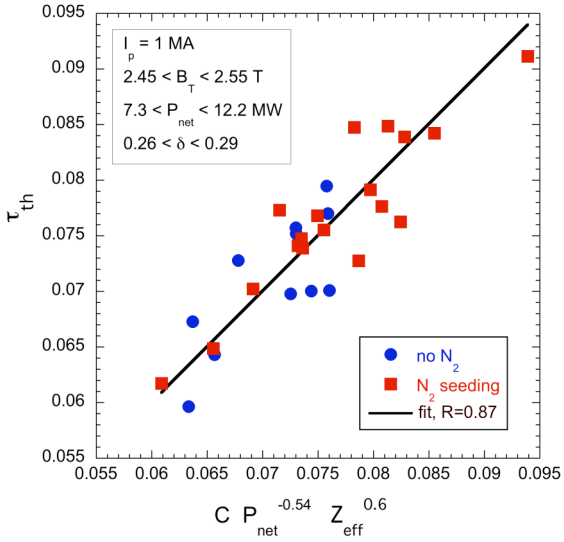

FIG. 7. Fit of thermal energy confinement τ_{th} for IPHMs of I_p =1MA and B_t=2.5T (dataset from 2008/9 where Z_{eff} values from IDA diagnostic were available). A power law Ansatz with heating power P_{net} and line-averaged Z_{eff}) leads to a good description of the data. The power degradation of confinement is less than in $H_{98(y,2)}$.

A strong correlation between local Z_{eff} values and the H_{98} factor for IPHMs with and without N_2 seeding was found in [14]. Here an attempt is made to highlight the important role of the Z_{eff} parameter for the scaling of the thermal energy confinement time τ_{th} (see fig. 7). Together with heating power P_{net} and the average Z_{eff} a power law fit to a subset of 2008/9 IMPH data was established which describes the experimental τ_{th} rather well. The weaker degradation of τ_{th} with P_{net} ($\propto P_{net}^{-0.54}$) compared to the H-mode scaling $H_{98(y,2)}$ ($\propto P_{net}^{-0.69}$) reflects the observed increase of H_{98} with β_N.

4. Gyro-kinetic simulations

The effect of nitrogen seeding on core confinement has been studied in a series of linear [10] and non-linear gyrokinetic simulations [11]. For the latter the GENE code was used for a scan of ∇T_i in both the seeded as well as the unseeded case taking experimental values for the other parameters like T_e, T_i, ∇n_e, q, Z_{eff} and magnetic shear. The TRANSP code was used to calculate ion and electron heat fluxes to provide an experimental reference to the simulations. For the N_2 seeded case a shift of the ITG critical R/L_{Ti} towards higher values was found to be caused by the mitigation of the ITG mode due to deuterium dilution. However, this effect, which would otherwise point to a core confinement improvement in the presence of N_2, is completely compensated by the observed higher $T_{e,i}$ values of N_2 seeded discharges, since the heat flux grows above the critical R/L_{Ti} as $T_i^{5/2}$. At the relevant heat fluxes simulated as well as experimental R/L_{Ti} values at both radial positions are similar for the seeded and for the unseeded case (see fig. 8). Thus, the predicted small relative change in R/L_{Ti} from the unseeded to the seeded case by the simulation is consistent with experimental findings. However, the cause for the discrepancy in absolute values of R/L_{Ti} vs. heat flux Q between simulation and experiment is still unclear and will be the target of future improved GENE simulation including also E x B shear effects.

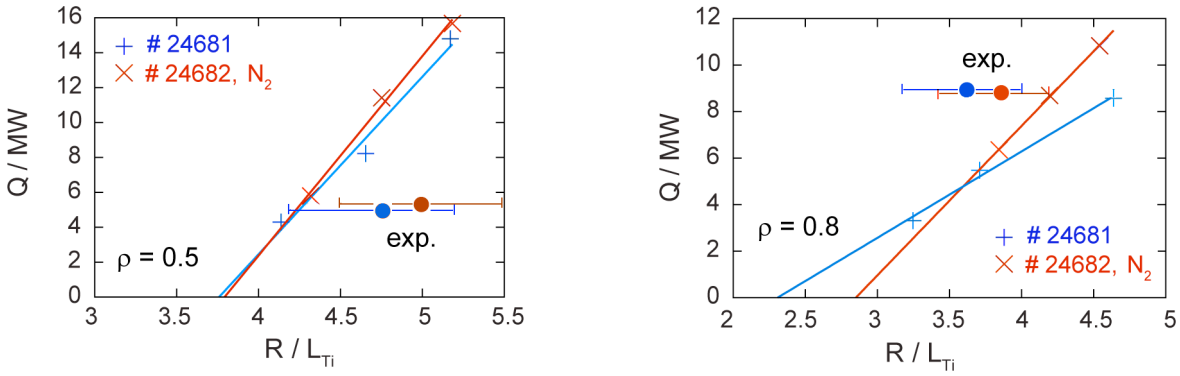

FIG. 8. Simulations with the non-linear gyrokinetic code GENE at two radial locations ρ_{tor} = 0.5 (left) and ρ_{tor} = 0.8 (right). The full symbols represent the heat flux Q reconstructed with TRANSP and R/L_{Ti} (w. error bars) from the measured profiles averaged over the respective flux surfaces.

5. Summary and Conclusions

In the 2008/9 campaigns high performance improved H-mode discharges were conducted with good energy confinement in particular when nitrogen was puffed with the primary goal of cooling the plasma edge. The achieved confinement factors H_{98} turned out to be as good as or even better than the ones obtained in the carbon dominated AUG when discharges at the same values of f_{GW} are compared. Thus, the compatibility of ITER relevant high confinement modes such as the improved H-mode or Hybrid scenario with an all-W wall has been strikingly demonstrated in ASDEX Upgrade. The improved confinement of N_2 seeded IPHMs is mainly an effect of higher pedestal temperatures which extend to the plasma core via profile stiffness. Gyrokinetic simulations support this picture. Peaking of the density profile in the presence of N_2 is weak and gives only a small contribution to the confinement improvement. Z_{eff} determined with improved methods turned out to be an important parameter to quantify the influence of nitrogen seeding on the energy confinement in the all-W AUG. Progress was also made with respect to extending the operational space of IPHMs in the all-W AUG towards lower q and higher plasma shape. However, this activity has just started and will be continued with more available ECRH power in the 2010/11 campaign. Also late heated IMPHs in the all-W AUG will be attempted for the first time in 2011. Still better confinement of IPHMs was found in previous AUG campaigns (< 2006) at lower ν^* only. This operational space is so far not accessible in the all-W AUG, but short and mid-term hardware improvements are hoped to improve the situation in this respect.

References

[1] STOBER, J., et al., Nucl. Fusion **47** (2007) 728
[2] NEU, R., for the ASDEX Upgrade team, Plasma Phys. Contr. Fus. **49** (2007) B59
[3] DUX, R., et al., this conference, IAEA-CN-180/EXD/6-2
[4] GRUBER, O., et al., Nucl. Fusion **49** (2009) 115014
[5] BOBKOV, V., et al. Nucl. Fusion **50** (2010) 035004
[6] HÖHNLE, H., et al., this conference, IAEA-CN-180/P7-25
[7] NEU, R., et al., this conference, IAEA-CN-180/P2-23
[8] KALLENBACH, A., et al., Plasma Phys. Contr. Fus. **52** (2010) 055002
[9] MAGGI, C. F., et al. Nucl. Fusion **50** (2010) 025023
[10] TARDINI, G., et al. presented at the 36th EPS Conference on Plasma Phys. Sofia, June 29 - July 3, 2009 ECA Vol.33E, O-2.004
[11] TARDINI, G., et al., 37th EPS Conference on Plasma Phys. Dublin, June 21-25, 2010
[12] MESSIAEN, A. M., et al., Nucl. Fusion, 34 (1994) 825
[13] GRUBER, O., et al., Phys. Rev. Lett. 74 (1995) 4217
[14] RATHGEBER, S. K., et al., Plasma Phys. Contr. Fus. **52** (2010) 095008